

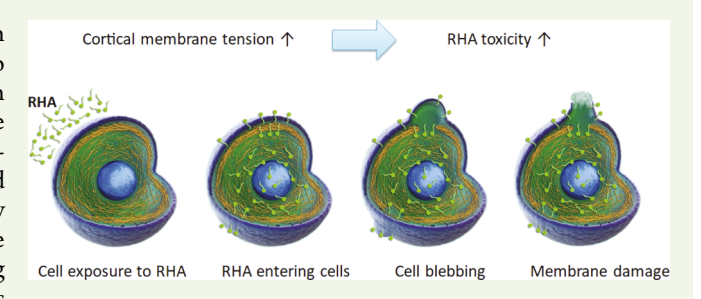
Cells with Higher Cortical Membrane Tension Are More Sensitive to Lysis by Biosurfactant Di-rhamnolipids

Chong Shen, [†] Lifang Jiang, [†] Xuwei Long, [†] Kris Noel Dahl, [‡] and Qin Meng*, [†]

[†]College of Chemical and Biological Engineering, Zhejiang University, 38 Zheda Road, Hangzhou, Zhejiang 310027, P. R. China [‡]Department of Chemical Engineering, Carnegie Mellon University, Doherty Hall 2100C 5000 Forbes Avenue, Pittsburgh, Pennsylvania 15213, United States

Supporting Information

ABSTRACT: Tissue and cellular stiffening is associated with pathologies including fibrosis and cancer. Healthy cells also exhibit a wide range of membrane cortical tensions, which have been studied in the field of mechanobiology. Here, we quantify the mechanosensitivity of the lysis agent the dirhamnolipid (RHA), which is a bacterially produced biosurfactant. RHA exhibited selective lysis correlated strongly with cortical membrane tension in osteoblasts, smooth muscle cells, fibroblasts, epithelial cells, and erythrocytes. Reducing cortical membrane tension by cytoskeleton inhibitors



(cytochalasin D and nocodazole) or osmotic regulators (sucrose, polyethylene glycol, and nonionic surfactants) attenuated the RHA toxicity. The selective toxicity of RHA toward human chronic myeloid leukemia K562 cells over healthy blood cells suggests a potential therapy for blood cancer. Targeted killing of myofibroblasts transformed from either fibroblasts or epithelial cells indicates its antifibrotic effect. Combined, these studies showed the potential for specific targeting of cells with differential mechanical properties rather than chemical or biological pathways.

KEYWORDS: cortical membrane tension, rhamnolipid, biosurfactant, myofibroblast, mechanosensitivity

1. INTRODUCTION

Each tissue in the body has a characteristic stiffness and tensional homeostasis varying from low values in blood to high values in muscles and bones. To balance tissue homeostasis, each cell has a unique optimal stiffness dominantly controlled by the cytoskeleton.² For example, differentiated myocytes and osteoblasts³ are several times stiffer than epithelial cells⁴ and 10-100 times more rigid than blood cells including monocytes, neutrophils, and erythrocytes.⁵

A drastic increase in tissue stiffness can be a hallmark of pathological fibrosis and cancer, which are generally detected by palpating the originally compliant tissue that has become a rigid mass.¹ Pathological cells in these rigid tissues, such as myofibroblasts in fibrotic tissues⁶ or cancer cells in mammary gland tumors, also exhibit significantly enhanced stiffness. Similarly, pathological cells in circulation systems, such as leukemia cells, parasite-infected red blood cells, or sickle cells, are several-to hundred-fold stiffer than their corresponding healthy cells.

Recently, targeting differential mechanical properties of cells has been suggested to provide a potential therapeutic advantage. For example, stiffening cell nuclei reduced the metastatic potential of cancer cells. The plasma membrane of cells is the easiest to target, and reducing membrane stiffness facilitates cell membrane resealing. Thus, we investigated if increasing cell stiffness would exacerbate cell damage because of membrane rupture.

The biosurfactant di-rhamnolipids (RHAs), produced by Pseudomonas aeruginosa, have already been accepted with pharmaceutical functions including regulating the immune system and 13 antibacterial 14 and possible anticancer properties. 15 In this article, we find that RHA causes a disproportionate rupture of stiffer cells. This finding may help to develop a novel and effective pharmaceutical application for treating organ fibrosis or tumor by selectively killing high-tensioned pathological cells.

2. MATERIALS AND METHODS

2.1. Cell Isolation and Culture. Human dermal fibroblasts were isolated from normal human foreskin of patients undergoing reconstructive surgery (approved by Zhejiang University, China) as described. 16 The fibroblasts were plated into T75 flasks for attachment culture with 10 mL of high-glucose Dulbecco's modified Eagle's medium (DMEM, Sigma-Aldrich, St. Louis, MO) supplemented with 10% fetal bovine serum (FBS, Gibco, Invitrogen Co. Ltd, Canada), 100 U/mL penicillin, and 100 μ g/mL streptomycin. Cultures between the third and fifth passages were used in all experiments.

Human neutrophils and erythrocytes were freshly isolated from whole blood drawn from healthy volunteers. Whole blood was layered on the upper-density gradient of a dual-density Percoll gradient

Received: August 23, 2019 Accepted: November 13, 2019 Published: November 13, 2019



ACS Biomaterials Science & Engineering

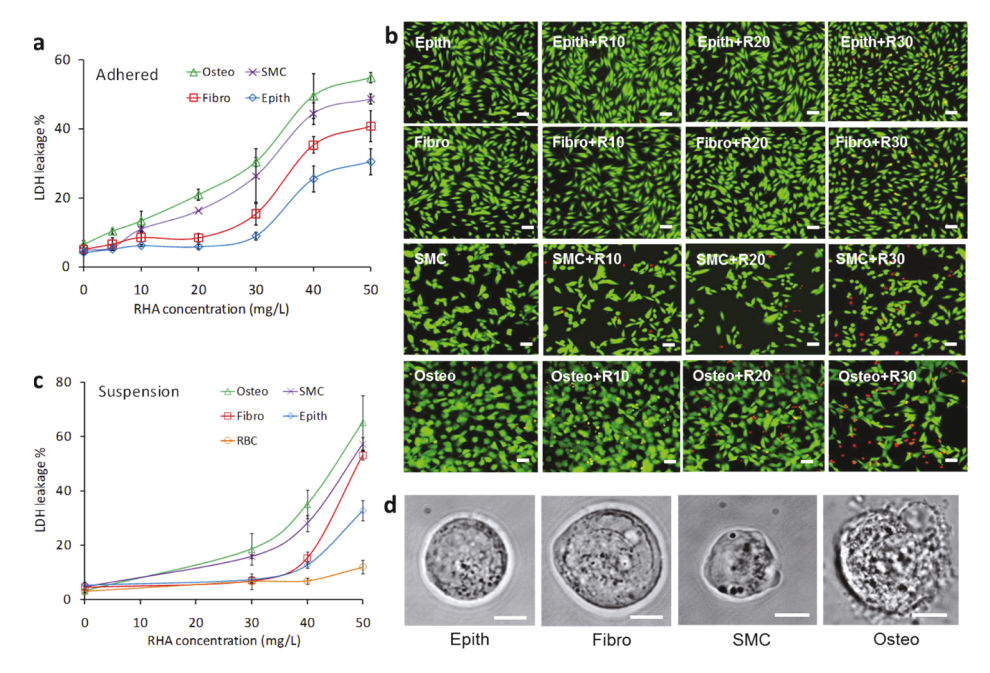


Figure 1. RHA toxicity for cells in suspension and attachment culture. (a) Cell viability represented by LDH leakage in attachment culture. *p < 0.05. (b) Calcein-AM/PI staining of live/dead cells in attachment culture. Scar bar: 20 μm. (c) Cell viability represented by LDH leakage in suspension culture. *p < 0.05. (d) Cell morphology after RHA treatment at 30 mg/L for 3–4 h in suspension culture. Scale bar: 5 μm. Osteo = Osteoblasts, SMC = smooth muscle cells, Fibro = fibroblasts, Epith = epithelial cells A549, and RBC = red blood cells.

created according to the manufacturer's instructions (Sigma-Aldrich, St. Louis, MO), and the solution was centrifuged at 2000 rpm for 30 min. The erythrocyte and neutrophil layers were sequentially collected, pelleted, and resuspended. The neutrophils were then incubated with sterile distilled water for 10 s to lyse red blood cell contaminants. Lysis was terminated by diluting with DMEM, and red blood cell ghosts were eliminated after centrifugation (Sigma-Aldrich, St. Louis, MO).

Epithelial A549 cells, osteoblast MC3T3-E1 cells, and a human smooth muscle cell (SMC) line were obtained from American Type Culture Collection (ATCC) and plated on T75 flasks for attachment culture in high-glucose DMEM with 10% FBS. K562 and K562/G cells were obtained from ATCC and suspended in Roswell Park Memorial Institute (RPMI) 1640 medium with 10% FBS for suspension culture in T75 flasks.

2.2. RHA Treatment and Cell Viability Assay. RHA is a gift from Zijing Bio. Inc., Huzhou, China, with purity > 99%, as described in Figure S1. The cells (AS49 cells, fibroblasts, osteoblasts, SMCs, neutrophils, erythrocytes, and K562 cells) were individually suspended for 6 h in DMEM containing 0.1% FBS and 0–50 mg/L RHA at 2×10^5 cells/mL. The attached cells of AS49 cells, fibroblasts, osteoblasts, SMCs were similarly treated with 0–50 mg/L RHA for 6 h in the same DMEM with 0.1% FBS.

Cell viability was measured by the lactate dehydrogenase (LDH) leakage assay. Briefly, the medium was sampled, and then the residual medium was removed from cells, which was washed twice with phosphate-buffered saline and lysed to release intracellular LDH of live cells into the new supernatant. LDH activities in the medium and cell lysate were determined using spectrophotometric methods that monitored the reduction of pyruvate with LDH assay kits (Saike Biotech. Inc, Ningbo, China). LDH leakage was calculated as the percentage of LDH in the medium versus the sum of LDH in the medium and in cells.

2.3. Assay on Cortical Membrane Tension. Cortical membrane tension was measured using a microfluidic device. The device was created using an SU-8 2050 photoresist film (Microchem, Newton, MA) and standard photolithography techniques (for design, see Figure S2). Cortical membrane tension was detected in cells resuspended in DMEM with 0.1% FBS, loaded into the inlet reservoir of the device, and conducting experiments automatically as described

in Figure S2. The cell suspension is driven by gravity with an applied pressure gradient (ΔP) equal to ρgh , where $\rho=1$ g/mL, g= the coefficient of gravity (9.8 m/s²), and h= the difference in liquid height between the inlet and outlet. The device was kept on a heating plate set at 37 °C. Experimental data were video-recorded under a microscope at 500 ms per frame.

2.4. Regulation of Cortical Membrane Tension. To reduce cortical membrane tension, cells were incubated with $10~\mu\mathrm{M}$ cytochalasin D (Sigma-Aldrich, St. Louis, MO) and $5~\mu\mathrm{M}$ nocodazole (Sigma-Aldrich, St. Louis, MO) for 1 h before treatment with 30 mg/L RHA or treated with 50 mM sucrose, $1000~\mathrm{mg/L}$ polyethylene glycol (PEG), $500~\mathrm{mg/L}$ Pluronic F127, or $200~\mathrm{mg/L}$ TWEEN 80 together with $30~\mathrm{mg/L}$ RHA. To increase cortical membrane tension, fibroblasts and $A549~\mathrm{cells}$ were first starved for $24~\mathrm{h}$ by incubating in FBS-free DMEM and then treated with $10~\mathrm{ng/mL}$ TGF- $\beta1~\mathrm{(Peprotech, Rocky Hill, NJ)}$ in DMEM-0.1% FBS medium for $72~\mathrm{h}$.

2.5. Cell Tracking Assay. Fibroblasts and myofibroblasts were labeled by CMFDA, green, and CM-DiI, red (both cell trackers from Thermo Scientific, Waltham, MA). After labeling, both cells were mixed 1:1 in DMEM containing 0.1% FBS. The cell mixture was seeded on 24-well plate at 1×10^5 cells/well. After overnight incubation, the culture medium was changed to DMEM with 0.1% FBS and 0, 20, and 30 mg/L of RHA.

2.6. Statistical Analysis. All data were analyzed by means \pm SD from three independent cell experiments. Data from multiple groups were compared using ANOVA in SPSS, or results from two different groups were compared with the unpaired Student *t*-test. P < 0.05 was considered statistically significant.

3. RESULTS AND DISCUSSION

3.1. RHAs Exhibit Specific Differential Cell Toxicities.

Osteoblasts (Osteo), SMCs, fibroblasts (Fibro), and epithelial cells (Epith) were treated with RHA in the media for 6 h. RHA treatment resulted in different necrotic responses (reflected by LDH leakage), with consistent membrane disruption across dosages Osteo > SMC > Fibro > Epith (Figure 1a,b and Table S1).

ACS Biomaterials Science & Engineering

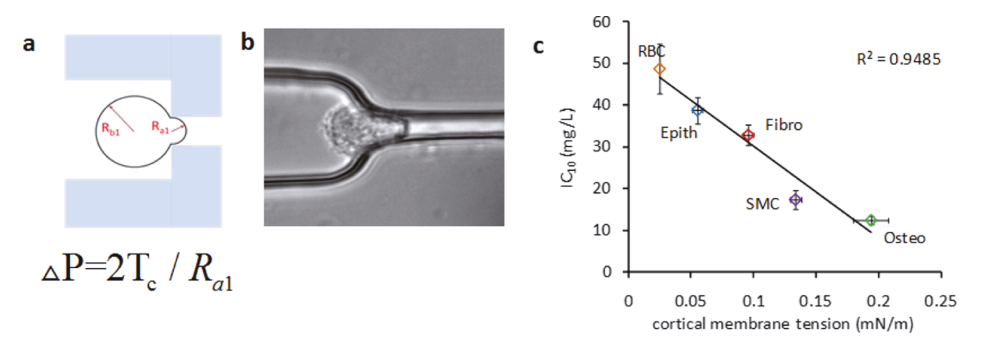


Figure 2. Relationship of cortical membrane tension to RHA toxicity of cells. (a) Sketch of an aspiration chamber to determine the stiffness of single cells. R_{a1} , R_{b1} : radii of cells aspirated into the micropipette. (b) RHA toxicity (IC₁₀) in suspension culture vs cortical membrane tension. Note: the membrane tension of RBC was obtained from a previous report.²⁰

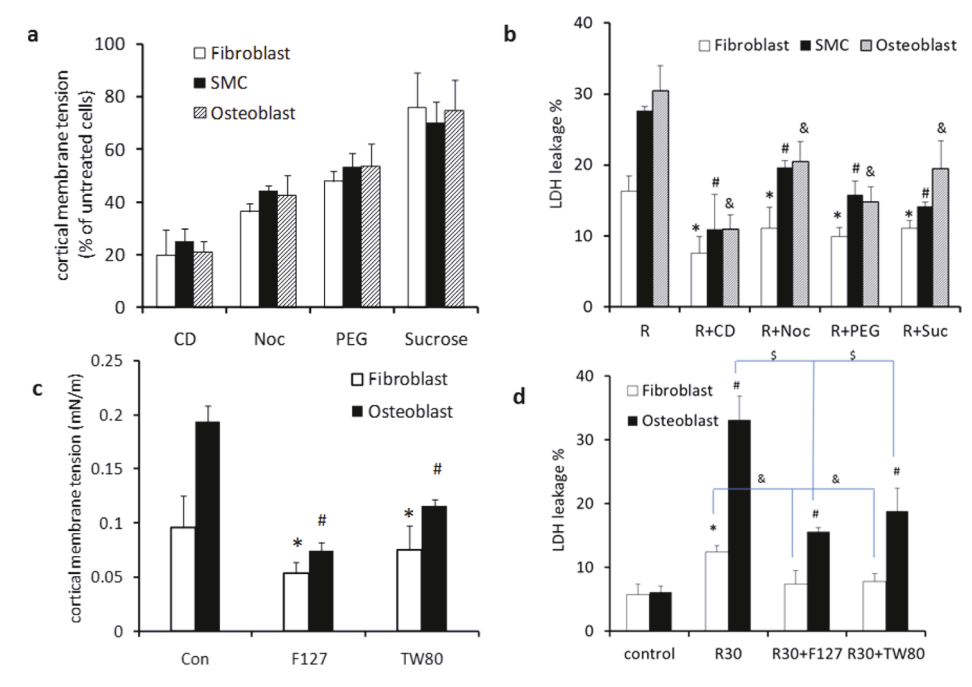


Figure 3. Effects of regulating cortical membrane tension on RHA toxicity of cells in suspension culture. (a) Cortical membrane tension is decreased by cytochalasin D (CD, $10 \mu M$), nocodazole (Noc, $5 \mu M$), PEG (0.1%), and sucrose (50 mM). (b) Toxicity of 40 mg/L RHA (R) is reduced by CD, Noc, PEG, and sucrose. (c) Cortical membrane tension is decreased by Pluronic F127 (500 mg/L) and TWEEN 80 (200 mg/L). (d) Toxicity of 40 mg/L RHA (R) is reduced by F127 and TWEEN 80. **,#,8 p < 0.05.

Cells grown in suspension were also considered to remove variability of cell—substrate attachment and cell—cell connectivity and for comparison with erythrocytes (also called red blood cells, RBC). In this case, the response of LDH leakage was Osteo > SMC > Fibro > Epith > RBC (Figure 1c). Higher resolution imaging of cells treated for 3–4 h of incubation with RHA at 30 mg/L showed that epithelial cells and fibroblasts maintained membrane integrity, whereas SMCs showed outward blebs and osteoblasts showed blebs and peripheral disruptions (Figure 1d).

3.2. Differential Cell Rupture from RHA Were Closely Correlated with Cortical Membrane Tension. As the surfactants have been known to elicit the cell rupture and necrosis via the interaction with cellular membranes, ¹⁷ the differential toxicity of RHA is possible to correlate with the cortical membrane tension of the different cells. As such, we measured effective cortical membrane tension of each cell in suspension culture using a simple, low-cost, and high-throughput technology ¹⁸ applying a microfluidic device (Figure 2a). To analyze the effective cortical membrane

tension, $T_{\rm C}$, we determined the pressure at which the radius of the aspiration length is approximately the radius of the pipette, which is engineered to be 2.5 μ m. We then calculated tension from a modified version of the Laplace equation (Figure 2a), wherein the material outside of the pipette is assumed to be an infinite space because it contains both a membrane reservoir and other mechanical elements that could bias the results (e.g., the nucleus and other organelles). A comparison of the $T_{\rm C}$ using the outer radius and the infinite model is shown in Figure S3.

When the cortical membrane tension of each cell is correlated with its RHA toxicity in suspension culture represented by IC_{10} , the two showed surprisingly good linearity ($R^2 = 0.949$) (Figure 2b).

3.3. RHA Toxicity Was Affected by Regulation of Cortical Membrane Tension. The cortical membrane tension was first modulated by the cytoskeleton-disrupting compounds of cytochalasin D and nocodazole or osmotic regulators (sucrose and PEG) (Figure 3a). As expected, the cortical membrane tension of osteoblasts, SMCs, and

ACS Biomaterials Science & Engineering

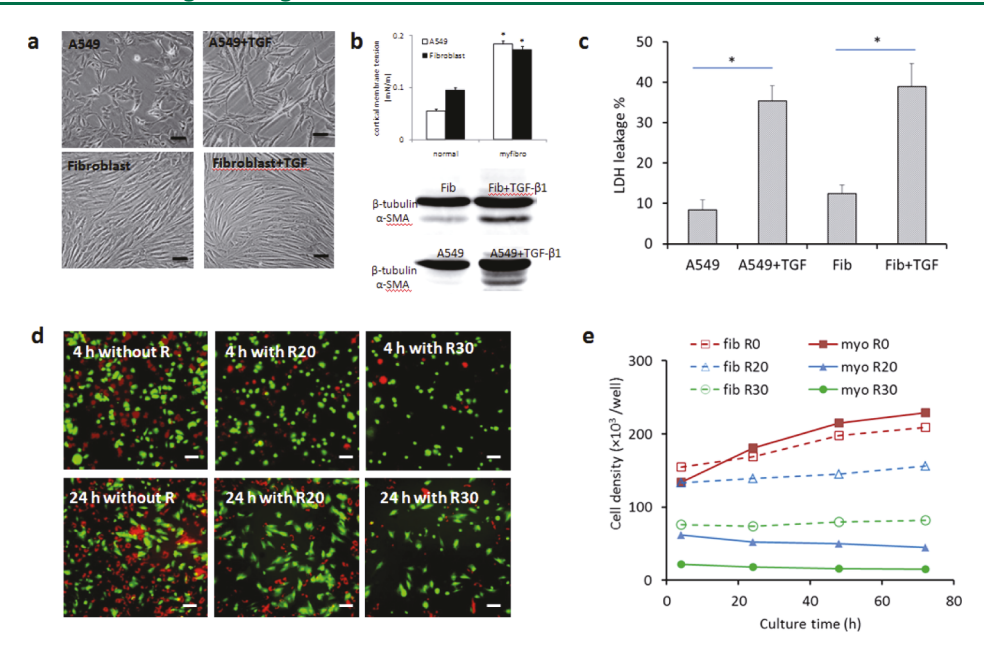


Figure 4. Selective toxicity of RHA on TGF- β 1-stimulated fibroblasts and A549 cells. (a) Changes in A549 and fibroblast morphology after TGF- β 1 treatment. (b) Enhanced cortical membrane tension and expression of α-SMA after TGF- β 1 treatment. *p < 0.05. (c) Enhanced RHA toxicity after TGF- β 1 treatment. *p < 0.05. (d) RHA treatment at 20 and 30 mg/L (R20 and R30, respectively) inhibits proliferation of myofibroblasts (red) transformed from fibroblasts (green). (e) Density of fibroblasts (fib) and myoblasts (myo) cultured with (20 and 30 mg/L) and without RHA. Scale bar = 20 μm.

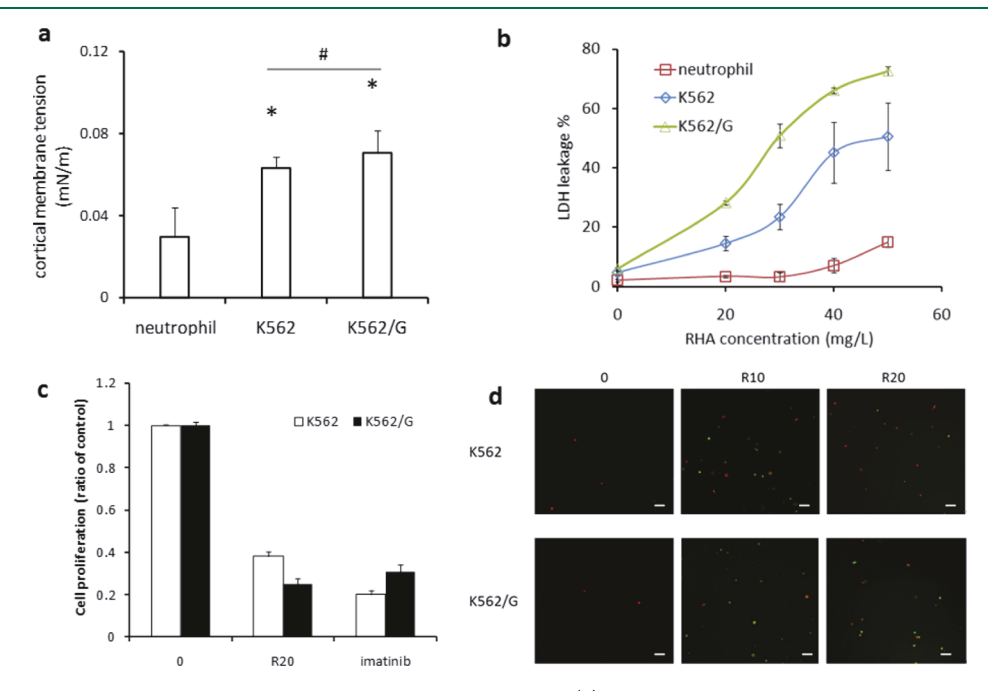


Figure 5. Selective toxicity of RHA on normal blood cells and blood cancer cells. (a) Cortical membrane tension of neutrophils and K562 cells. (b) RHA toxicity in neutrophils and K562 cells. (c) Inhibition of K562 proliferation by RHA at 20 mg/L after 48 h of exposure, while imatinib at 1 mg/L was set as the control. (d) Cell apoptosis induced by RHA at 10 and 20 mg/L.

fibroblasts was reduced, with cytochalasin D showing the most potent effect because of its ability to prevent the cell from regulating cortical membrane tension and disassemble the cortex from the plasma membrane. Similarly, all these treatments significantly attenuated the damage of RHA toward the three cell types, with cytochalasin D being the most effective (Figure 3b). Comparison of Figure 3a,b shows that reducing cortical membrane tension significantly improved cell survival after the RHA treatment. Similarly, Pluronic F127 or TWEEN 80, which apparently lowered cortical membrane

tension (Figure 3c), also attenuated RHA-induced cell damage (Figure 3d), exhibiting protection against cell death similar to that of the surfactant Pluronic F68.¹¹

3.4. Potential Application of RHA for Treating Fibrotic Diseases. Fibrotic diseases occur in many organs such as liver, lung, and kidney, where myofibroblasts as dominant pathological cells persist and excrete collagen, replacing the functional parenchyma of the organ and contributing to organ stiffening. The selective killing of myofibroblasts with high cortical membrane tension offers a

potential approach to developing robust and effective therapies for treating fibrotic diseases. As shown in Figure 4a,b, transforming fibroblasts or A549 epithelial cells into myofibroblasts, respectively, increased membrane cortical tension 1.8- and 3.3-fold, accompanied by the increased expression of α -smooth muscle actin.

As expected, more severe cell necrosis was observed in myofibroblasts that showed higher cortical membrane tension when treated with RHA (Figure 4c). This finding was confirmed in a cell-tracking system where green fibroblasts and red myofibroblasts transformed from fibroblasts were mixed together. After treatment with 20 and 30 mg/L RHA, the population of red myofibroblasts decreased more dramatically than green fibroblasts (Figure 4d). This cell selectivity was confirmed by quantifying the cell proliferation that decreased greatly in myofibroblasts than in fibroblasts (Figures 4e and S4).

As a common feature of fibrosis, myofibroblasts should become important therapeutic targets, but their precise origins are complex and differ in varying organs. For example, myofibroblasts in kidney fibrosis arise via differentiation from local resident fibroblasts (50%), bone marrow (35%), endothelial-to-mesenchymal transition program (10%), and epithelial-to-mesenchymal transition program (5%).²² Nevertheless, the current treatment strategy is mainly to block the transformation of myofibroblasts from epithelial or endothelial cells²³ using compounds such as simvastatin,²⁴ IL-10,²⁵ and caffeine, 26 which only suppress a small fraction of myofibroblasts. Hence, no specific treatments are yet available to control fibrosis and preserve organ function. In contrast, RHA may provide a robust and effective treatment by directly targeting myofibroblasts with less toxicity to neighboring normal cells. Our recent finding that the RHA showed effective preventive function against the scar formation on rabbit ears²⁷ could provide a support in verifying the specific function of RHA in potentially treating fibrotic organs.

3.5. Potential Application of RHA for Treatment of Blood Cancer. The relationship between cell stiffness and RHA toxicity was further examined in blood cancer cells of human chronic myeloid leukemia K562 cells. As shown in Figure 5a, the cortical membrane tension of K562 and K562/G (an imatinib-resistant strain) was measured to be over onefold greater than that of neutrophils isolated from normal human blood (see Materials and Methods). K562 and K562/G cells showed greater sensitivity (more LDH leakage) to RHA toxicity than neutrophils and erythrocytes (Figures 5b and 1c). Culture of cells in the presence of 20 µg/mL RHA greatly inhibited the proliferation of K562 cells (Figure 5c). Interestingly, the RHA at this level could effectively inhibit the proliferation of K562 and K562/G to the levels of that of the clinical treatment of imatinib. The greater sensitivity of human myeloid leukemia K562 cells to RHA suggests its function against blood cancer, whose cells are characterized by greater cortical membrane tension⁹ than healthy blood cells. The specificity of RHA treatment could directly eliminate pathological cancer cells in flow without requiring complicated sorting devices.

The potential effects of RHA on solid tumors remain unclear and should be confirmed by in vivo experiments. Currently available solid tumor cell lines generally fail to retain their original phenotype, ²⁸ particularly deviating from their biological behavior in traditional two-dimensional cultures by losing integrins that are activated to generate tension force

when they encounter a mechanical rigid matrix or are exposed to an exogenous force.¹ Tumor cells, which naturally exhibit greater cell stiffness than normal cells in situ, became much softer immediately after isolation⁴ and some of them after many passages in vitro become even softer than normal cells.¹ Thus, we strongly recommend that the possible anticancer function of RHA should be explored in vivo or in well-organized three-dimensional cultures where tumor cells recapitulate the original tumor phenotype as much as possible.

4. CONCLUSIONS

In summary, the biosurfactant RHA selectively kills tensioned cells in the order of decreasing toxicity with decreasing cortical membrane tension: osteoblasts > SMCs > fibroblasts > epithelial cells > erythrocytes. RHA toxicity was attenuated by reducing cortical membrane tension, but enhanced by increasing cortical membrane tension. These findings have a potential therapeutic value for fibrosis and blood cancers.

ASSOCIATED CONTENT

S Supporting Information

The Supporting Information is available free of charge at https://pubs.acs.org/doi/10.1021/acsbiomaterials.9b01305.

Structure of RHA; microfluidic for the cortical membrane tension measurement; calculation of $T_{\rm C}$ by different models; and toxicity of RHA on different cells (PDF)

AUTHOR INFORMATION

Corresponding Author

*E-mail: mengq@zju.edu.cn. Phone: +86-571-8795-3193. Fax: +86-571-8795-1227.

ORCID

Chong Shen: 0000-0002-0606-6989 Xuwei Long: 0000-0002-8586-7425 Qin Meng: 0000-0002-8017-6852

Notes

The authors declare no competing financial interest.

ACKNOWLEDGMENTS

We gratefully acknowledge financial support for this study from the NSFC (National Natural Science Foundation of China, no. 21776242) and the NSF (National Science Foundation, no. 1634888 to KND).

REFERENCES

- (1) Butcher, D. T.; Alliston, T.; Weaver, V. M. A tense situation: forcing tumour progression. *Nat. Rev. Cancer* **2009**, *9*, 108–122.
- (2) Schaefer, A.; Hordijk, P. L. Cell-stiffness-induced mechanosignaling a key driver of leukocyte transendothelial migration. *J. Cell Sci.* **2015**, *128*, 2221–2230.
- (3) Wyss, K.; Yip, C. Y. Y.; Mirzaei, Z.; Jin, X.; Chen, J.-H.; Simmons, C. A. The elastic properties of valve interstitial cells undergoing pathological differentiation. *J. Biomech.* **2012**, *45*, 882–887.
- (4) Lopez, J. I.; Kang, I.; You, W.-K.; McDonald, D. M.; Weaver, V. M. In situ force mapping of mammary gland transformation. *Integr. Biol.* **2011**, *3*, 910–921.
- (5) Hochmuth, R. M. Micropipette aspiration of living cells. *J. Biomech.* **2000**, 33, 15–22.
- (6) Schneider, D.; Baronsky, T.; Pietuch, A.; Rother, J.; Oelkers, M.; Fichtner, D.; Wedlich, D.; Janshoff, A. Tension monitoring during epithelial-to-mesenchymal transition links the switch of phenotype to

- expression of moesin and cadherins in NMuMG cells. PLoS One 2013, 8, No. e80068.
- (7) Rosenbluth, M. J.; Lam, W. A.; Fletcher, D. A. Force microscopy of nonadherent cells: a comparison of leukemia cell deformability. *Biophys. J.* **2006**, *90*, 2994–3003.
- (8) Guo, Q.; Reiling, S. J.; Rohrbach, P.; Ma, H. Microfluidic biomechanical assay for red blood cells parasitized by Plasmodium falciparum. *Lab Chip* **2012**, *12*, 1143–1150.
- (9) Sosale, N. G.; Rouhiparkouhi, T.; Bradshaw, A. M.; Dimova, R.; Lipowsky, R.; Discher, D. E. Cell rigidity and shape override CD47's "self"-signaling in phagocytosis by hyperactivating myosin-II. *Blood* **2015**, *125*, 542–552.
- (10) Ribeiro, A. J. S.; Khanna, P.; Sukumar, A.; Dong, C.; Dahl, K. N. Nuclear stiffening inhibits migration of invasive melanoma cells. *Cell. Mol. Bioeng.* **2014**, *7*, 544–551.
- (11) Togo, T.; Alderton, J. M.; Bi, G. Q.; Steinhardt, R. A. The mechanism of facilitated cell membrane resealing. *J. Cell Sci.* **1999**, *112*, 719–731.
- (12) Togo, T.; Krasieva, T. B.; Steinhardt, R. A. A decrease in membrane tension precedes successful cell-membrane repair. *Mol. Biol. Cell* **2000**, *11*, 4339–4346.
- (13) Piljac, G.; Piljac, V. Immunological activity of rhamnolipids. Comp. Immunol. Microbiol. Infect. Dis. 1998, 21, 5.
- (14) Sotirova, A. V.; Spasova, D. I.; Galabova, D. N.; Karpenko, E.; Shulga, A. Rhamnolipid-biosurfactant permeabilizing effects on grampositive and gram-negative bacterial strains. *Curr. Microbiol.* **2008**, *56*, 639–644.
- (15) Christova, N.; Tuleva, B.; Kril, A.; Georgieva, M.; Konstantinov, S.; Terziyski, I.; Nikolova, B.; Stoineva, I. Chemical structure and in vitro antitumor activity of rhamnolipids from Pseudomonas aeruginosa BN10. *Appl. Biochem. Biotechnol.* **2013**, *170*, 676–689.
- (16) Garner, W. L.; Karmiol, S.; Rodriguez, J. L.; Smith, D. J., Jr.; Phan, S. H. Phenotypic differences in cytokine responsiveness of hypertrophic scar versus normal dermal fibroblasts. *J. Invest. Dermatol.* **1993**, *101*, 875–879.
- (17) Jiang, L.; Shen, C.; Long, X.; Zhang, G.; Meng, Q. Rhamnolipids elicit the same cytotoxic sensitivity between cancer cell and normal cell by reducing surface tension of culture medium. *Appl. Microbiol. Biotechnol.* **2014**, *98*, 10187–10196.
- (18) Zheng, Y.; Nguyen, J.; Wei, Y.; Sun, Y. Recent advances in microfluidic techniques for single-cell biophysical characterization. *Lab Chip* **2013**, *13*, 2464–2483.
- (19) Boal, D. Mechanics of the Cell; Cambridge University Press, 2012
- (20) Hale, J. P.; Winlove, C. P.; Petrov, P. G. Effect of hydroperoxides on red blood cell membrane mechanical properties. *Biophys. J.* **2011**, *101*, 1921–1929.
- (21) Tinevez, J.-Y.; Schulze, U.; Salbreux, G.; Roensch, J.; Joanny, J.-F.; Paluch, E. Role of cortical tension in bleb growth. *Proc. Natl. Acad. Sci. U.S.A.* **2009**, *106*, 18581–18586.
- (22) LeBleu, V. S.; Taduri, G.; O'Connell, J.; Teng, Y.; Cooke, V. G.; Woda, C.; Sugimoto, H.; Kalluri, R. Origin and function of myofibroblasts in kidney fibrosis. *Nat. Med.* **2013**, *19*, 1047–1053.
- (23) Tomasek, J. J.; Gabbiani, G.; Hinz, B.; Chaponnier, C.; Brown, R. A. Myofibroblasts and mechano-regulation of connective tissue remodelling. *Nat. Rev. Mol. Cell Biol.* **2002**, *3*, 349–363.
- (24) Yang, T.; Chen, M.; Sun, T. Simvastatin attenuates TGF- β 1-induced epithelial-mesenchymal transition in human alveolar epithelial cells. *Cell. Physiol. Biochem.* **2013**, *31*, 863–874.
- (25) Shi, J.-H.; Guan, H.; Shi, S.; Cai, W.-X.; Bai, X.-Z.; Hu, X.-L.; Fang, X.-B.; Liu, J.-Q.; Tao, K.; Zhu, X.-X.; Tang, C.-W.; Hu, D.-H. Protection against TGF-β1-induced fibrosis effects of IL-10 on dermal fibroblasts and its potential therapeutics for the reduction of skin scarring. *Arch. Dermatol. Res.* **2013**, 305, 341–352.
- (26) Arauz, J.; Galicia-Moreno, M.; Cortés-Reynosa, P.; Salazar, E. P.; Muriel, P. Coffee attenuates fibrosis by decreasing the expression of TGF-beta and CTGF in a murine model of liver damage. *J. Appl. Toxicol.* **2013**, 33, 970–979.

- (27) Shen, C.; Jiang, L.; Shao, H.; You, C.; Zhang, G.; Ding, S.; Bian, T.; Han, C.; Meng, Q. Targeted killing of myofibroblasts by biosurfactant di-rhamnolipid suggests a therapy against scar formation. *Sci. Rep.* **2016**, *6*, 37553.
- (28) Ince, T. A.; Sousa, A. D.; Jones, M. A.; Harrell, J. C.; Agoston, E. S.; Krohn, M.; Selfors, L. M.; Liu, W.; Chen, K.; Yong, M.; Buchwald, P.; Wang, B.; Hale, K. S.; Cohick, E.; Sergent, P.; Witt, A.; Kozhekbaeva, Z.; Gao, S.; Agoston, A. T.; Merritt, M. A.; Foster, R.; Rueda, B. R.; Crum, C. P.; Brugge, J. S.; Mills, G. B. Characterization of twenty-five ovarian tumour cell lines that phenocopy primary tumours. *Nat. Commun.* **2015**, *6*, 7419.